

## Experimental Studies of Zonal Flows in CHS and JIPPT-IIU

A. Fujisawa, K. Itoh, H. Iguchi, K. Matsuoka, S. Okamura, A. Shimizu, T. Minami, Y. Yoshimura, K. Nagaoka, C. Takahashi, M. Kojima, H. Nakano, S. Ohshima, S. Nishimura, M. Isobe, C. Suzuki, T. Akiyama, K. Ida, S.-I. Itoh<sup>1</sup> and P. H. Diamond<sup>2</sup>, CHS group.

Y. Hamada, A. Nishizawa, T. Ido, T. Watari, K. Toi, Y. Kawasumi and JIPPT-IIU group.

*National Institute for Fusion Science, Oroshi-cho, Toki, Japan 509-5292*

<sup>1</sup>*RIAM, Kyushu Univ., Kasuga, Japan 816-8580*

<sup>2</sup>*University of California, San Diego, La Jolla, California, U. S. A., 92093-0319*

e-mail: fujisawa@nifs.ac.jp

**Abstract.** Zonal flow is now one of central topics for transport study in toroidal plasmas, and its detection is a challenging experimental subject. This paper introduces trials to identify zonal flows in toroidal plasmas, i.e., CHS and JIPPT-IIU, with HIBPs. The main results are the first confirmation of the existence of residual zonal flows, and findings of coherent oscillations that can be the Geodesic Acoustic Modes in CHS and JIPPT-IIU.

### 1. Introduction

Plasma turbulence has been studied for over a half century as a mechanism to govern the transport in toroidal plasmas. One of the successful achievements in this field is that the shear of mean radial electric field (or perpendicular flow) can suppress turbulence and transport to result in improved confinement modes [1-4]. Recently, the other players in regulating plasma transport, *zonal flows* [5,6], have come into the transport study in toroidal plasmas. The importance of zonal flow study becomes crucial to give a precise prediction of the plasma transport, in particular, the performance of International Thermonuclear Experimental Reactor (ITER) [7-9].

The zonal flows can be driven exclusively by nonlinear interactions with turbulence, on the other hand, the meso-scopic structure of zonal flows has an effect on plasma turbulence through time-varying ExB shearing. Direct nonlinear simulations have, in fact, confirmed the mutual interaction between zonal flows and turbulence, and their essential role in turbulence and transport [10-16]. However, only a few experimental trials have been performed to identify zonal flows and their effects on confinement [17-23].

In toroidal plasmas, two major branches of zonal flows are expected, i.e., a residual flow of nearly zero frequency, and an oscillatory flow termed Geodesic Acoustic Modes (GAMs) [24,25]. These zonal flows appear in electric field fluctuation symmetric ( $m=n=0$ ) on magnetic flux surface with finite radial wave numbers. Hence, direct measurement of electric field is essential to identify the zonal flows. Advantageously, heavy ion beam probes (HIBP) are able to measure electric field of the plasma interior. This paper presents the first experimental detection, using the HIBPs, of the residual zonal flows in CHS [26], together with findings of coherent oscillation presumed as GAMs in CHS [26] and JIPPT-IIU [27].

### 2. Heavy Ion Beam Probe

In the diagnostics, the energy difference between injected and detected beams corresponds to the plasma potential at the ionization point. Hence, the fluctuation of the

beam energy represents to the potential fluctuation. Besides, the fluctuation of detected beam intensity gives information of density fluctuation, as

$$\tilde{I}_{\text{det}}/I_0 = \tilde{n}_e/n_e - \int \tilde{n}_e S_1 dl_1 - \int \tilde{n}_e S_2 dl_2, \quad (1)$$

where  $I_0$ ,  $S_1$ , and  $S_2$  mean the initial beam intensity, electron impact ionization cross-section from singly ionized state to the others, and the one from doubly charged state to the others, respectively. The local density fluctuation can be estimated from that of the detected current fluctuation (i.e.,  $\tilde{I}/I_{\text{det}} \approx \tilde{n}_e/n_e$ ), if the plasma density is sufficiently low to neglect the integral terms.

Heavy ion beam probes are often capable to simultaneously measure several adjacent points of plasma along the beam orbit. Difference between potentials at two channels gives a measure of electric field, i.e.,  $E\delta r = -(\phi(\rho_2) - \phi(\rho_1))$ . The potential fluctuation at a point  $\rho_2$  can be written by electric field fluctuation and potential fluctuation at an adjacent position  $\rho_1$  along the orbit in a symbolic manner,

$$\tilde{\phi}(\rho_2) = -\tilde{E}\delta r + \tilde{\phi}(\rho_1) \approx -\tilde{E}\delta r + \int_a^{\rho_1} \tilde{E} dl, \quad (2)$$

Consequently, potential fluctuation should contain the integrated fluctuation of electric field along the beam orbit, similarly to the path integral effects of density fluctuation. Therefore, the local electric field measurement is superior in the detection of the zonal flows, although the measurements need higher signal-to-noise ratio than that of potential fluctuation.

### 3. Experimental Results of CHS

#### 3-1. Experimental Conditions

The Compact Helical System (CHS) is a helical device with the major and minor radii being  $R=1.0\text{m}$ ,  $a=0.20\text{m}$ , respectively. The magnetic field strength of CHS is up to 2T. The CHS is equipped with two HIBP systems. As is shown in Fig. 1(a), the locations of two HIBPs are apart approximately by 90 degree in the toroidal direction. Both HIBPs have almost the same geometrical characteristics with their maximum energy of 200keV. Each of them is capable to measure three adjacent positions in the plasma. The necessary beam energy is  $\sim 70$  keV, using cesium, for this magnetic field strength of 0.88T in order to see the plasma center.

The experiments were performed in plasmas produced with electron cyclotron resonance heating of  $\sim 200$  kW. The plasma parameters are, magnetic field strength  $B=0.88$  T, density  $n_e \sim 5 \times 10^{12} \text{cm}^{-3}$ , electron temperature  $T_e \sim 1\text{keV}$ , ion temperature  $T_i \sim 0.1$  keV, ion Larmor radius  $\rho_i \sim 0.1\text{cm}$ , time scale of micro-instabilities  $\Omega^* \sim 50\text{kHz}$  with  $k_{\text{perp}}\rho_i \sim 0.3$  and energy confinement time  $\tau_E \sim 2.5\text{ms}$  (or the characteristic frequency  $\tau_E^{-1}/2\pi \sim 0.1\text{kHz}$ ).

#### 3-2. Spectra of potential and electric field fluctuations

Electric field fluctuation has been measured with dual HIBPs. Figure 1(b) shows a spectrum of the electric field fluctuation, and its coherence between two toroidal locations; here potential difference,  $E\delta r = -(\phi(\rho_2) - \phi(\rho_1))$ , is just termed '*electric field*' for simplicity. The observed radial location is  $r_{\text{obs}} = 12 \pm 0.5$  cm, or two thirds of plasma minor radius. Here, the Fast Fourier Transform (FFT) technique is applied for sequential windows taken from the stationary period of  $\sim 80$  ms. Spectrum in Fig. 1(b) is a shot-average of the ensembles. The signal-to-noise ratio for the measurement is the maximum since detected beam current is largest around the observation point. The fluctuation in the low frequency range ( $< \sim 1\text{kHz}$ ) shows a high coherence ( $\sim 0.6$ ) between two toroidal locations. The coherence can become

closer to one in an appropriate period of a single shot. The fluctuation with the long-range correlation in this frequency regime should represent the residual zonal flow.

For comparison, Fig. 1(c) shows the corresponding spectrum of potential fluctuation, and coherence between potentials. Their characteristics are obviously different in power and coherence. Particularly, in the frequency range from 1 kHz to 10 kHz, the potential fluctuation power is much larger than that of the electric field as the frequency is lower. The potential power decreases as  $P \sim f^{-1.9}$ , while the power of electric field as  $P \sim f^{-0.6}$  in the range from  $\sim 1$  kHz to  $\sim 10$  kHz. On the other hand, the coherence of power is quite high around  $\sim 2$  kHz ( $\sim 0.9$  at the maximum). The difference in power and coherence suggests presence of significant coherent fluctuations with this low frequency range in outer region of the observation radius.

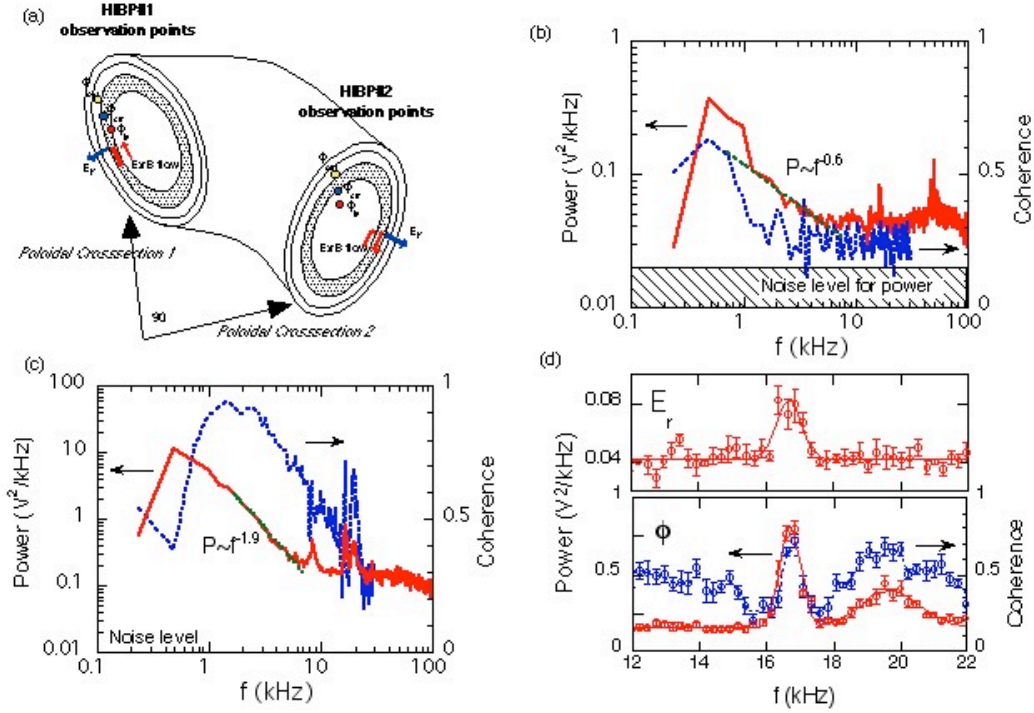


Figure 1. (a) Geometry of dual heavy ion beam probes on CHS, (b) Fluctuation spectrum of electric field and coherence between two toroidal locations. The hatched region represents noise level of measurements of electric field fluctuation power. (c) Power and coherence in potential fluctuation. (d) Expanded views of power spectrum of electric field fluctuation (upper), and power spectrum of potential and coherence between potentials (lower).

Figure 1(d) shows expanded views around the peak for power spectra of potential and electric field, and coherence in potential between two toroidal locations. In the power spectrum of electric field shows a sharp peak at  $f \sim 16.5$  kHz with a width of  $\sim 1$  kHz. On the other hand, the power spectrum of potential fluctuation, two peaks at  $f \sim 16.5$  and  $f \sim 20.0$  kHz can be found. These peaks show quite high coherence up to  $\sim 0.8$ , although a significant coherence cannot be evaluated owing to the poorer signal-to-noise ratio for electric field fluctuation. In this experimental condition, the theoretically expected GAM frequency is  $c_s/2\pi R \sim 17$  kHz, with  $c_s$  being the ion sound velocity. Consequently, the prediction of frequency and long-range correlation suggests that the electric field fluctuation of  $f \sim 16.5$  kHz should represent a GAM.

The other peak at  $f \sim 20$  kHz could be also a GAM, which is interfused into potential fluctuation due to the effect of electric field integral (in Eq. (2)). This mode should be located

on an outer region of the observation point ( $r_{\text{obs}} \sim 12$  cm), owing to its absence in spectrum of electric field fluctuation. The sharpness of both peaks in potential suggests that ‘GAM’ may have eigenmode-like characteristics in localization and frequency. Otherwise, the ‘GAM’ should appear as broader band structure in potential spectrum owing to its dependence on temperature varying with radius.

### 3-2. Spatio-temporal Structure of Residual Zonal Flow

The electric field fluctuation of  $f < \sim 1$  kHz shows a long-range correlation. The fluctuation, the residual zonal flows, can be extracted by using a numerical filter. The numerical filter is defined as  $\phi_f(t) = \int_{t-\infty}^{t+\infty} f(t-t')\phi(t')dt'$  with  $f(t-t') = \left(1/\sqrt{2\pi\tau_f^2}\right)\exp[-(t-t')^2/2\tau_f^2]$ . The time constants for high and low frequency cut-off are selected here as  $\tau_f = 0.3$  ms and  $\tau_f = 1.0$  ms, respectively. The extremely low frequency is removed to avoid the effects of plasma movement or changes in plasma. The filter property has a peak around 0.5 kHz with the width of  $\sim 1$  kHz in frequency domain. This property corresponds to the coherence curve indicated in Fig. 1(b).

Figures 2(a) and (b) shows examples of the processed electric field. In the case of Fig. 2(a), the observation points of dual HIBPs are located on the same magnetic flux surface, while the observation points in Fig. 2(b) are located in slightly different magnetic flux surfaces. The waveforms of both cases alter temporally in a synchronized way. Obviously, the former and the latter cases show phase difference of  $\sim 0$  and  $\sim \pi/2$ , respectively. No phase-shift of this fluctuation on a magnetic flux surface demonstrates the toroidal symmetry ( $n=0$ ) of electric field fluctuation. The fact also supports the poloidal symmetry ( $m=0$ ), with an assumption that the electric field is constant on a magnetic field line (see ref. [26] in detail). On the other hand, a finite phase shift in Fig. 2(b) indicates that the coherent fluctuation should have a radial structure.

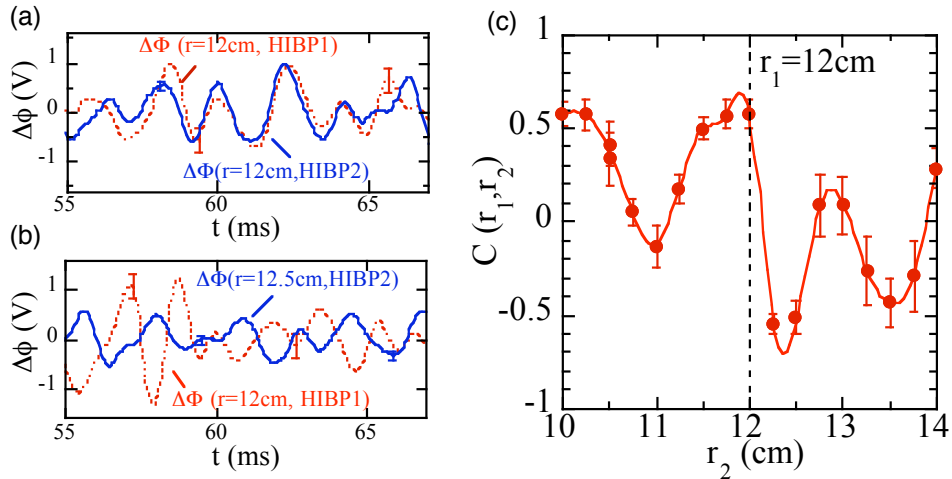


Figure 2. Spatio-temporal structure of residual zonal flows in CHS. (a) Waveforms of electric fields at two toroidal locations,  $\Delta\phi$ , on the same flux magnetic surface. (b) Those on slightly different magnetic flux surfaces. (c) Radial structure of zonal flows represented in cross-correlation coefficients.

The radial structure can be inferred as follows. The electric field fluctuation could be expressed as  $E(r) = -\tilde{E}_z(r) - \tilde{E}_r(r)$ , where the  $E_z$  and  $E_r$  represent the residual zonal flow

and the others, respectively. An analysis using cross-correlation technique can give a rough radial structure of the zonal flow;  $C(r_1, r_2) = \langle \mathbf{E}(r_1) \cdot \mathbf{E}(r_2) \rangle / \sqrt{\langle \mathbf{E}^2(r_1) \rangle \langle \mathbf{E}^2(r_2) \rangle}$ , where  $\langle \rangle$  means the time-average. Supposed that  $\tilde{E}_z(r) = E_z \cos(k_r r - \omega t)$  and  $E_T/E_z$  is sufficiently small, the correlation function is reduced to  $C(r_1, r_2) \cong (1 - E_T^2/E_z^2) \cos k_r(r_1 - r_2)$ . Dual HIBP systems allow us to perform this manner of analysis. The result, shown in Fig. 2(c), demonstrates that the electric field fluctuation (or residual zonal flow) should have a radial structure with the dominant wavelength of  $\sim 1$ cm. These results provide clear evidence to show existence of electric field fluctuation symmetric on a magnetic flux surface, with finite radial wavelength, that is, zonal flow.

## 4. Experimental Results of JIPPT-IIU

### 4-1. Experimental Conditions

JIPPT-IIU is a tokamak with the major and minor radii being 0.93m and 0.23m, respectively. The maximum field strength is 3T. The JIPPT-IIU is equipped with a single HIBP. The maximum energy of this HIBP is 500 keV. An excellent feature with this HIBP is that the system has multiple channels available (6 at maximum) to observe adjacent positions in the poloidal cross-section of the plasma. Figure 3a illustrates sets of observation points for three different values of beam energy; 450 keV, 300keV and 250 keV. Neighboring five or six marks represent a set of observation points that can be observed simultaneously.

The experiments are performed in ohmically heated plasmas with toroidal current of 200kA. The safety factor is about 4.3 at the edge, and the plasma density  $1 \times 10^{13} \text{ cm}^{-3}$  and the central electron temperature about 1keV.

### 4-2. Fluctuation Spectra and Correlation Analysis

The potential fluctuation measurements revealed the existence of coherent activity of potential in the core region of the plasma. Figure 3(b) is an example of potential fluctuation spectra. The spectrum shows the existence of a peak around  $\sim 45$  kHz with the width of  $\sim 5$  kHz. The observation points are indicated by an arrow in Fig. 3(a); the normalized minor radius of the observed location is  $\rho \sim 0.2$ , and an expanded view of the observed points is shown as the inset.

In this case, the coherent activity is found in all of four observation points; those are located within  $\pm 1$ cm around the central magnetic flux surface. The cross-correlation functions of these points are shown in Fig. 3(c). Every function shows quite similar characteristics. These curves are well fitted with the function of  $C(\tau) = C(0) \exp(-\tau/\tau_{\text{Decay}}) \cos(2\pi f\tau)$  with almost the same parameters;  $C(0) \sim 0.8$ ,  $\tau_{\text{Decay}} \sim 55 \mu\text{s}$ , and  $f \sim 46 \text{ kHz}$ . The feature suggests the poloidal (or  $m=0$ ) symmetry of the modes, if the integral effects are neglected (see Eq. (2)). In the measurements on other sets of multiple observation points, a tendency is found that the correlation could decrease as the observation points become aligned in radial direction. This tendency suggests that the high correlation may not be simply ascribed to the integral effects of electric field fluctuation.

The measurements of the coherent activities in potential were performed for other sets of observation points. The survey allows us to investigate the radial dependence of the amplitude and the frequency of the oscillatory mode. The dependences are shown in Fig. 3(d). It is easily found that both amplitude and frequency increases toward the core. This tendency is quantitatively consistent with the theoretical expectation of GAM frequency,  $f \sim c_s/R$ . The

increase of the amplitude could be related to the decrease of flow damping rate (i.e., ion-ion collisionarity) toward the core. These facts qualitatively support that the oscillation could be GAM.

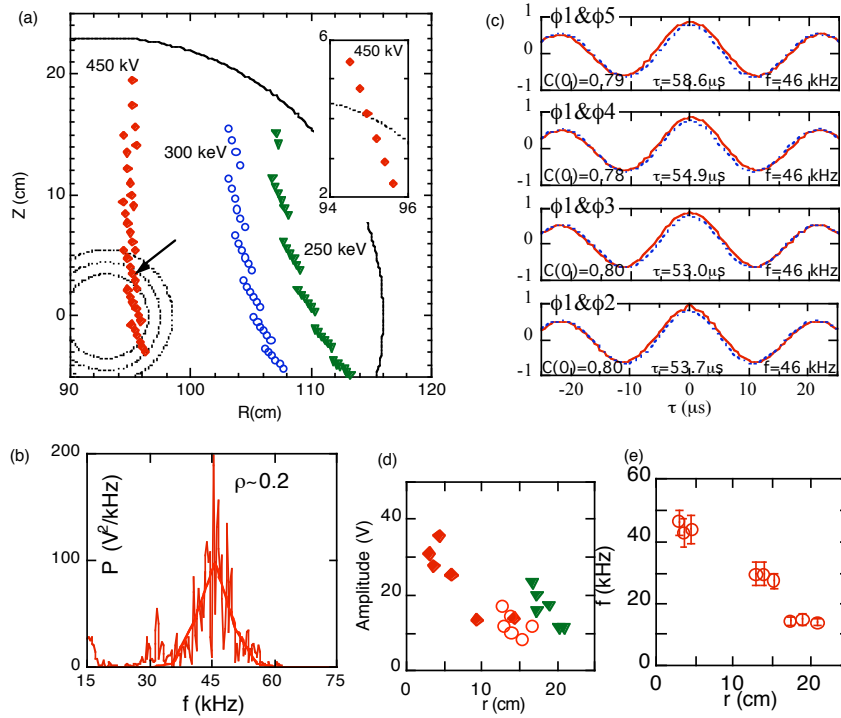


Figure 3. (a) Sets of observation points of HIBP on JIPPT-IIU for three different beam energies (450 keV, 300 keV, 250 keV). The inset shows an expanded view of the set of observation points (the centers of gravity) indicated by the arrow. (b) Potential fluctuation spectrum at the observation point indicated by the arrow in Fig. 3(a). (c) Cross-correlations (red lines) between channels. The dashed blue lines represent the fitting curves. The numbers ( $C(0)$ ,  $\tau_{\text{Decay}}$ ,  $f$ ) are the fitting parameters used for the curve. (d) The radial dependence of the amplitude of coherent oscillation, and (e) The radial dependence of frequency.

## 5. Discussion and Summary

### 5-1. Zonal Flows and Confinement

Zonal flow and turbulence can be regarded as a system that exchanges energy between them. Then, energy distribution between zonal flow and turbulence can be an important factor to determine plasma confinement since the symmetrical characteristics of zonal flow cannot contribute to any radial transport. Therefore, an increase in zonal flow energy should result in better improvement. In CHS, a result is available to show a relation between zonal flow, turbulence and confinement. In other words, a clear difference is found between the amplitude of the zonal flow among cases with and without a transport barrier [28].

Figure 4 shows an example of a change in zonal flow amplitude before and after a back-transition. In Fig. 4(a), two waveforms of potential are shown; one indicates clear transition feature at  $t \sim 70$  ms, while the other shows no change at that time. This means that the former HIBP observes a point inside the barrier. Besides, the detected beam intensities of the latter HIBP around the central channel show opposite characteristics; the inside signal rises but the outside decreases at the transition time. The fact strongly suggests that the central channel of the latter HIBP should be exactly located on the barrier foot-point.

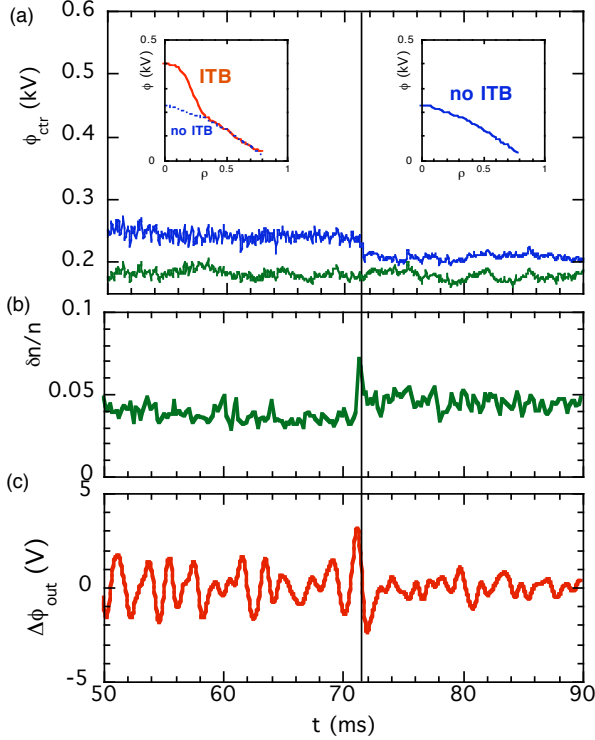


Figure 4. Change in zonal flows and fluctuation with and without transport barrier. (a) Waveforms of potentials at the barrier foot point and barrier inside. The insets show potential profiles before and after the transition. (b) Waveforms of density fluctuation, and (c) waveforms of amplitude of zonal flow at the barrier.

absolute value of zonal electric field is  $0.05\sim 0.1$  kV/m, with an assumption of volume distance being  $\Delta r_{eff} \sim 1.5$  cm. The amplitude of zonal flow seems rather small, although the absolute value can become a factor larger by taking into account the beam focusing property and a finite size of sample volumes. On the other hand, the huge amplitude of ‘GAM’ in JIPPT-IIU can give a much larger zonal electric field.

The smaller value of the residual zonal flow in CHS, could be ascribed to the flow damping mechanism due to the inhomogeneity of magnetic field (or large parallel viscosity). Actually, the charge exchange recombination spectroscopic measurements confirmed that the toroidal flows driven by parallel-injected neutral beam are quite small compared to those of tokamaks [29]. This feature, large damping rate of zonal flow, can explain the different characteristics in transport between tokamaks and the helical device. In this sense, the symmetry of magnetic configuration can be a key factor to design plasma confinement devices with high confinement performance.

### 5-3. Summary

In summary, we have introduced the HIBP measurements in NIFS. One of the major achievements in the measurements is to show the presence of the residual zonal flows and their fundamental characteristics in CHS. This is the first identification of the residual zonal flow in a toroidal plasma. Besides, the other branch of zonal flow, GAM, is suggested to exist in CHS and JIPPT-IIU. The experimental confirmation of existence of zonal flows should

Figures 4b and Fig 4c show the density fluctuation (in the frequency range of more than  $f \sim 2$  kHz) and zonal flow amplitudes in the HIBP at the barrier foot point, respectively. After the back-transition, the zonal flow amplitude decreases with a simultaneous increase in the density fluctuation amplitude. Note that the relative increase in the local density fluctuation after the back-transition can be actually larger if the path integral effect is taken into account. As a result, this observation indicates that large energy distribution to zonal flow could be a cause of confinement improvement in the barrier region. Also this result may - the ITB characterized by stronger zonal flow - suggest an important role of an interplay between zonal flow and turbulence fluctuation in transport.

### 5-2. Viscosity and zonal flows

According to the waveforms in Figs. 2(a) and (b), the observed amplitude of the residual zonal flow is  $\sim 1$  V. The

enhance the prospect of plasma burning in the ITER. The presented works, trial for the identification of zonal flows, are the prologue to start a new age of plasma turbulence research.

### Acknowledgements

This work is partially supported by the Grant-in-Aids for Scientific Research (No. 15360497) and Specially-Promoted Research (No. 16002005). The authors also express a great appreciation to Director General O. Motojima and Prof. Emeritus M. Fujiwara for their continuous encouragements and supports.

### References

- 1) Yoshizawa, A. , Itoh, S. -I., Itoh, K., ‘Plasma and Fluid Turbulence’ (Institute of Phys. Pub., Bristol and Philadelphia, 2003).
- 2) Biglari, H., Diamond, P. H., Terry, P. W., Phys. Fluids B **2** 1 (1990);
- 3) Itoh, S.-I., and Itoh K., J. Phys. Soc. Jpn. **59**, 3815 (1990).
- 4) Hasegawa A., Maclennan, C. G., and Kodama, Y., Phys. Fluids **22**, 2122 (1979)
- 5) Diamond, P. H. *et al*, in Proceedings of the 17th IAEA fusion energy conference, Yokohama, 1998 **vol. 4** 1421-1428.(International Atomic Energy Agency, Vienna, Austria, 1999).
- 6) Diamond, P. H., Itoh, K., Itoh, S.-I., Hahm, T. S., Plasma Phys. Control. Fusion in press.
- 7) Glanz, J., Science **274**, 1600 (1996).
- 8) Lin, Z., Hahm, T. S., Lee, W. W., Tang, W. M., White, R. B., Science **281**, 1835 (1998).
- 9) Rosenbluth, M. N., Hinton, F. L., Phys. Rev. Lett. **80**, 724 (1998).
- 10) Hasegawa, A., Wakatani, M., Phys. Rev. Lett. **59**, 1581 (1987).
- 11) Hammet, G., et al., Plasma Phys. Control. Fusion **35**, 973 (1993).
- 12) Waltz, R. E., Kerbel, G. D., Milovich, J., Phys. Plasmas **1**, 2229 (1994)
- 13) Dimits, A. M., et al., Phys. Plasmas **7**, 969 (2000).
- 14) Hallatshek, K., Phys. Rev. Lett. **84**, 5145 (2000).
- 15) Scott, B. D., Phys. Plasmas **7**, 1845 (2000).
- 16) Watanabe, T. -H., Sugama, H., Phys. Plasmas **9**, 3659 (2002).
- 17) Hamada, Y., et al., Fusion Eng. Design **34-35**, 663 (1997).
- 18) Schoch, P. M., Connor, K. A., Demers, D. R., Zhang, X., Rev. Sci. Instrum. **74** 1846 (2003).
- 19) Shats, M. G., Solomon, W. M., Phys. Rev. Lett. **88**, 045001 (2002).
- 20) Xu, G.S. et al., Phys. Rev. Lett. **91**, 125001 (2003)
- 21) McKee, G. R. *et al.*, Plasma Phys. Control. Fusion **45**, A477 (2003).
- 22) Moyer, R. A., Tynan, G. R., Holland, C., Burin, M. J., Phys. Rev. Lett. **87**, 135001 (2001).
- 23) Diamond, P. H., *et al.* Phys. Rev. Lett. **84**, 4842 (2000).
- 24) Winsor, N., Johnson, J. L., and Dawson, J. M., Phys. Fluids **11**, 2448 (1968).
- 25) Hallatshek, K., Biskamp, D., Phys. Rev. Lett. **86** 1223 (2001).
- 26) Fujisawa, A., et al., Phys. Rev. Lett. in press.
- 27) Hamada, Y. et al., submitted to Nucl. Fusion.
- 28) Fujisawa, A., *et al.* Phys. Rev. Lett. **82**, 2669(1999).
- 29) Ida, K., Yamada, H., Iguchi H., et al., Phys. Rev. Lett. **67** 58(1991).